Available online at www.sciencedirect.com
ScienceDirect
Carbohydrate Polymers 69 (2007) 363–370
Carbohydrate Polymers
www.elsevier.com/locate/carbpol

Interactions between *N*-succinyl-chitosan and bovine serum albumin

Ai-ping Zhu [a,*], Lan-hua Yuan [a], Tian Chen [a], Hao Wu [a], Feng Zhao [b]

[a] *College of Chemistry and Chemical Engineering, Yangzhou University, Yangzhou, 225002, PR China*
[b] *Department of Chemical and Biomedical Engineering, Florida State University, Tallahassee, FL 32310, USA*

Received 7 October 2006; received in revised form 9 November 2006; accepted 24 November 2006
Available online 16 February 2007

Abstract

Interactions between proteins and biocompatible amphiphilic chitosan derivatives have been investigated owing to their scientific and technological importance. In this study, the interactions between *N*-succinyl-chitosan (NSCS) and bovine serum albumin (BSA) are characterized by circular dichroism (CD); isothermal titration calorimetric (ITC); ultraviolet (UV) spectrum; fluorescence spectrum and transmission electron microscopy (TEM) techniques. ITC has been used to demonstrate that BSA binds to NSCS with a molar ratio of 30:1. The binding isotherms for these H-bond and hydrophobic interactions are exothermic. The CD and Fluorescence spectrum indicate that the conformation of BSA does not change significantly during the chain entanglements between BSA and NSCS. The NSCS entrapped BSA shows a nanosphere morphology revealed by TEM techniques. This study demonstrates the potential for NSCS matrix encapsulation of proteins or other hydrophilic bioactive drugs.

Keywords: *N*-succinyl-chitosan; Bovine serum albumin; Conformation; Interactions

1. Introduction

Production of pharmaceutically active peptides and proteins in large quantities has become feasible (Liang et al., 2004). The oral route is considered to be the most convenient way of drug administrations for patients. Nevertheless, the intestinal epithelium is a major barrier to the absorption of hydrophilic drugs such as peptides and proteins (Borchard et al., 1996). This is because hydrophilic drugs can not diffuse across the cells through the lipid-bilayer membrane.

Polymeric nanoparticles have been widely investigated as a carrier for drug delivery. There are several advantages of nanoparticles over microspheres (Soma, Dubernet, Bentolila, & Benita, 2000). It has been observed that the number of nanoparticles that traverse the epithelium is greater than the number of microspheres breaching the epithelium. Due to their good biocompatibilty much attention has been paid to nanoparticles made of synthetic biodegradable polymers such as poly-ε-caprolactone and polylactide (Guzman, Aberturas, Rodriguez-Puyol, & Molpeceres, 2000; Wehrle, Magenheim, & Benita, 1995). However, these nanoparticles are not ideal carriers for hydrophilic drugs because of their hydrophobic properties. In addition, the procedures for preparation of biodegradable polymeric nanoparticles are complex and use harmful solvents. It is known that organic solvents may cause degradation of peptide or protein drugs that are unstable or sensitive to their environments (Kajihara et al., 2001).

Chitosan (CS), a cationic polysaccharide, is derived from chitin by alkaline deacetylation (Chen et al., 2004). It was reported that CS is nontoxic and soft-tissue compatible (Iwasaki et al., 2004; Jin, Song, & Hourston, 2004). Additionally, it is known that chitosan has a special feature for adhering to the mucosal surface and transiently opening the tight junctions between epithelial cells (Artursson, Lindmark, Davis, & Illum, 1994). Therefore, chitosan has received much attention for delivery of therapeutic peptides, proteins, antigens, oligonucleotides and genes by intravenous, oral and mucosal administration (Calvo,

* Corresponding author. Tel.: +86 514 7975568; fax: +86 514 7975524.
E-mail address: apzhu@yzu.edu.cn (A. Zhu).

0144-8617/$ - see front matter © 2007 Published by Elsevier Ltd.
doi:10.1016/j.carbpol.2006.11.023

Remunan-Lopez, Vila-Jato, & Alonso, 1997; Dureja, Tiwary, & Gupta, 2001; Hu et al., 2002; Kofuji, Ito, Murata, & Kawashima, 2001; Mao et al., 2001; Roy, Mao, Huang, & Leong, 1999; Xu & Du, 2003). Calvo et al. first developed these nanoparticles, using a tripolyphosphate cross-linking method, to be used as protein carriers (Calvo et al., 1997); hydrophobically modified chitosan can aggregate into the nanoparticles, which is used as a matrix to contain trypsin (Liu, Desai, Chen, & Park, 2005). Mumper (Liu, Zhang, Sun, Sun, & Yao, 2003) was the first to propose delivery of a gene into a cell using chitosan as a vector. The results reveal that it is hard for naked DNA to enter the cell membrane due to electrostatic shielding. Whereas chitosan or chitosan derivatives facilitate DNA entry into the cell membrane due to the perturbation caused by electrostatic and hydrophobic interactions. Most commercially available CSs have a quite large molecular weight (Mw) and need to be dissolved in an acetic acid solution at a pH value of approximately 4.0. However, the modified chitosan has a good solubility at a pH value close to physiological pH. Loading of peptide or protein drugs at physiological pH ranges may prevent their bioactivity from decreasing. *N*-succinyl-chitosan (NSCS), a kind of biocompatible chitosan derivative, can self-assembly into regular nanospheres in distilled water (Zhu, Chen, Yuan, Wu, & Lu, 2006). The NSCS nanospheres are obtained under very mild conditions without the need of high temperature, organic solvents, surfactants or other special experimental technology (Zhu et al., 2006), which avoids the degradation of peptide or protein caused by organic solvents. The biopolymeric matrixes are thought to influence the activity of bioactive drugs and proteins, but the nature of molecular-scale interactions of biopolymers with bioactive macromolecules are poorly understood.

In this study, the interactions between NSCS and BSA were characterized by circular dichroism (CD); isothermal titration calorimetric (ITC); ultraviolet (UV) spectrum; fluorescence spectrum and transmission electron microscopy (TEM) techniques. Our results demonstrate that chain entanglements are easily formed between NSCS and BSA and mainly driven by H-bond and hydrophobic interactions. The conformation of BSA entrapped in the matrix of NSCS does not change significantly, suggesting that NSCS is a potential matrix to load proteins or other hydrophilic bioactive drugs.

2. Experimental

2.1. Materials

Chitosan powder was supplied by Lianyungang Biologicals Inc., China, which has a deacetylation degree of 90% and viscosity average molecular weight of 20,000 D. All commercially available solvents and reagents used were of analytical grade and no further purifications were made. BSA was purchased from fraction V, Sigma–Aldrich.

2.2. Synthesis of N-succinyl-chitosan (NSCS)

The synthesis of NSCS (Scheme 1) was performed according to our recent report (Zhu et al., 2006), in detail: 1 g chitosan was dissolved into 200 ml 1 wt% HAc solution and then transferred into a flask. Succinic anhydride (0.2 g) was dissolved in acetone (20 ml) and added into the flask drop-wise for 30 min at room temperature, and then the reaction was allowed stirred for 4 h at 40 °C. The reaction mixture was cooled to room temperature. The mixture precipitated in an excess of acetone. The precipitates were filtered to remove the solvent and then washed with 70%, 80%, 100% acetone, respectively. Finally, the product was dried at 40 °C under vacuum conditions for 24 h. The obtained white powder (NSCS) weighed 1.1 g.

2.3. Fluorescence and UV spectroscopy

The intrinsic fluorescence properties of the proteins were studied on an F-4500 (Hitachi high-technologies corporation, Tokyo, Japan) spectrometer with a 3 ml quartz cell with a 1 cm path length. The concentration of BSA in all of the experiments was kept at 0.33 mg/ml. The concentration of NSCS was varied from 0.0125 to 0.25 mg/ml in the solutions. The excitation and emission slit widths were fixed at 5 nm. The excitation wavelength was set at 295 nm to selectively excite the tryptophan molecules, and the emission spectra were monitored in the wavelength range of 315–390 nm. The emission spectra of BSA–NSCS solutions were subtracted from the distilled water–NSCS blanks, and the average of three accumulated scans was recorded as the final graph. The UV spectrum was measured by a UV-2501PC (Shimadzu corporation, Japan) spectrometer.

2.4. Circular dichroism measurements

Circular dichroism (CD) spectroscopy (J-810, JASCO corporation, Japan) was used to measure the conformation change of BSA encapsulated into NSCS with respect to the native one. The BSA and BSA/NSCS solutions were scanned over the wavelength range 200–260 nm, using a 5 mm quartz cylindrical cell. The secondary structures of native BSA and BSA entrapped in NSCS were evaluated by comparing the α-helix content, corresponding to the ellipticity of the bands at 208 nm. Since α-helices are one of the elements of secondary structure, the quantitative analysis of structural change of BSA could be evaluated by the content of the α-helix preserved. The α-helix content of proteins is estimated according to the following equation (Greenfield & Fasman, 1969):

$$\%\alpha - \text{Helixcontent} = \frac{\theta_{\text{mrd}} - 4000}{33000 - 4000} \quad (1)$$

where, θ_{mrd} is the mean molar ellipticity per residue at 208 nm (deg cm^2 dmol^{-1}). Usually the raw data from the experiment are expressed in terms of θ_{d} (the ellipticity in

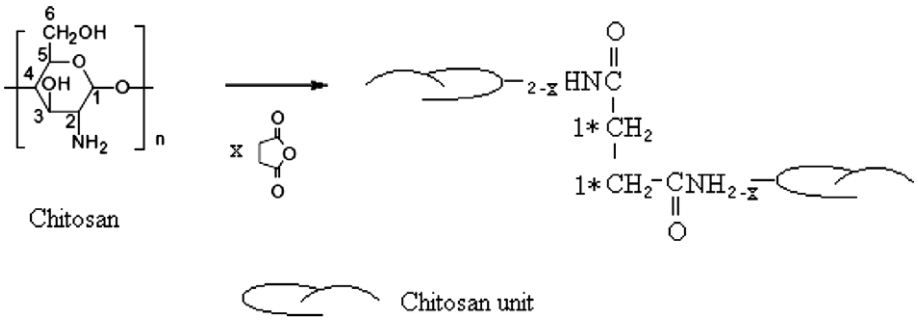

Scheme 1. Synthesis of NSCS.

the unit of mdeg). However, it can be converted to mean molar ellipticity per residue, using the following equation:

$$\theta_{\mathrm{mrd}} = \frac{\theta_{\mathrm{d}} M}{10 C L N_{\mathrm{r}}} \quad (2)$$

where, M is the BSA molecular weight (Da), C is the BSA concentration (mg/ml), L is the sample cell path length (cm), and N_{r} is the number of amino residue.

2.5. Isothermal titration calorimetry

The isothermal titration calorimetric experiments were carried out on a VIP-ITC (Microcal Inc., Northampton, MA). All of the solutions were thoroughly degassed before loading, and the consequent water loss was made up with degassed deionized water. Titrations were carried out using a 250 μl autopipet at 300 rpm stirring speed. The sample cell (approximately 1.439 mL) was loaded with the distilled water or the 0.025 mg/ml of NSCS solutions, and the autopipet was filled with 1 mg/ml BSA solution. The cells are both insulated by an adiabatic shield. The titration was carried out at 25.0 ± 0.02 °C. This power compensation, differential instrument was previously described in detail by Wiseman et al. (Jelesarov & Bosshard, 1999; Wiseman, Williston, Brandts, & Lin, 1989). The calorimetric data were analyzed using the MicroCal Origin 7.0 software provided with the instrument. The enthalpy change for each injection was calculated by integrating the area under the peaks of the recorded time course of change of power and then subtracted with control titrations.

2.6. Morphology characterization

The morphology of the BSA encapsulated in the NSCS matrix was measured using transmission electron microscopy (TEM) techniques. The specimens were prepared by dropping the sample solution onto a copper grid. The grid was held horizontally for 20 s to allow the molecular aggregates to settle and then at 45° to allow excess fluid to drain for 10 s. The grid was returned to the horizontal position, and one drop of 2% phosphotungstic acid was added to give a negative stain. The grid was then allowed to stand for 30 s–1 min before excess staining solution was removed by draining as above. The specimens was air-dried and examined using a (TE CHAI-12) (philips) transmission electron microscope at an accelerating voltage of 80.

3. Results and discussion

3.1. UV spectrum

Fig. 1 shows the UV spectrum of BSA in different of NSCS concentrations. According to literature (Kandori, Uoya, & Ishikawa, 2002), the large absorption peak at 275 nm appears due to phonyl group of tryptophan residues (Trp) and tyrosines. From this figure, it can be seen that all the peaks in different NSCS concentrations do not show any shift, however, the intensity is strongly dependant on the NSCS concentrations. The UV intensity increases at low concentration (Such as 0.0125, 0.025 and 0.05 mg/ml) of NSCS, while decreases at high concentration (Such as 0.125, 0.175 and 0.25 mg/ml) of NSCS.

As shown in Scheme 1, there are hydrophilic groups such as –NH–CO– and –OH and hydrophobic moieties, such as $–CH_2CH_2–$, acetyl groups and glucosidic rings on NSCS macromolecules. Due to the amphiphilic property of NSCS, it can form hydrophobic domains, in which, hydrophobic Trps and tyrosines residues are easy to

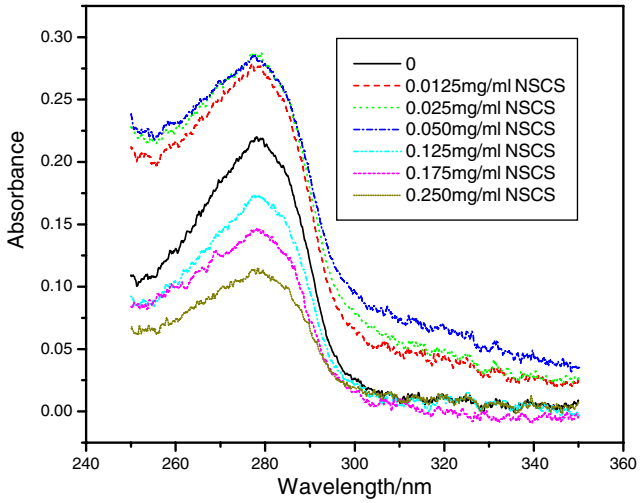

Fig. 1. UV spectrum of BSA in different concentrations of NSCS (BSA concentration was kept at 0.33 mg/ml).

dissolve. As a result, the intensity of the UV peak for BSA increases with an increase of the NSCS concentration in the range of low concentrations (<0.05 mg/ml) of NSCS. By further increasing NSCS concentration, the intensity decreases inversely, obviously in comparison with that of the pure BSA solution. The intensity becomes lowest at the highest concentration of NSCS. The decrease in intensity may be caused by the formation of complexes between NSCS and BSA due to the interchain hydrophobic associations, causing the more hydrophilic microenvironment around the residues of Trps and tyrosines. The similar phenomenon is also found by Gao, Wang, Fan, and Ma (2006) that "The complex interactions of the modified CyDs with BSA lead to an altered solute–environment interaction and thus decrease the UV absorbance in the spectrum of BSA."

3.2. Fluorescence spectroscope

Intrinsic fluorescence is used to assess the structural changes of BSA during interaction with NSCS. The emission spectra of pure BSA and BSA in different concentrations of NSCS solution are depicted in Fig. 2. In BSA, there is a tryptophan (Trp) residue, which is one of the three natural occurring aromatic amino acid residues, fluorescing when excited with UV light. The fluorescence is usually dominated by the contribution of the Trp. Because both their absorbance at the excitation wavelength and their quantum yield emission are considerably greater than the respective values for tyrosine and phenylalanine. When a BSA molecule undergoes the conformation change, the Trp residue is exposed to the environment and therefore affects the fluorescence. The fluorescence of Trp in BSA varies with its conformational change and shows a blue shift of the emission maximum wavelength (λ_{em}) (Kasai, Horie, Mizuma, & Awazu, 1987; Walton & Maenpa, 1979).

From Fig. 2, the fluorescence intensity at λ_{em} of Trp is not shifted with increasing the NSCS concentration. The result may indicate that the conformation of BSA does not change in NSCS solutions. However, the fluorescence intensity of Trp decreases in all concentrations of NSCS solution, which is not always consistent with the case of UV spectrum. That is possible because the UV and fluorescence peaks are produced by different contributions of residues of BSA, fluorescence peak is usually related to Trps, while UV peak is dependant not only on the two Trps but also 19 tyrosines. From the present results, it can be concluded that the Trps residues more easily produce the hydrophobic associations within NSCS in comparison with that of tyrosine residues, at low concentrations of NSCS. The hydrophobic interactions between BSA and NSCS create chain entanglements, causing the changes of the microenvironment around Trps residues and decreasing the fluorescence intensity of BSA with increasing NSCS concentration.

3.3. Circular dichroism (CD)

In addition to the fluorescence spectrum, circular dichroism (CD) techniques have proved to be an alternative effective method to measure the conformational transitions of a protein. It can provide useful information such as the content changes of the α-helix structure and secondary structure involving β-sheet components (Magzoub, Kilk, Eriksson, Langel, & Graslund, 2001; Militello, Vetri, & Leone, 2003; Peng, Hidajat, & Uddin, 2004). Fig. 3 shows the CD spectrum of BSA dependant on the NSCS concentrations. The characteristic peaks at 208 and 222 nm, respectively, are ascribed to the α-helix structure.

Proteins are organized by different levels of structure, such as primary, secondary, tertiary and quaternary structures. The primary structure is the chemical structure of the polypeptide chain or chains in a given protein, i.e., the

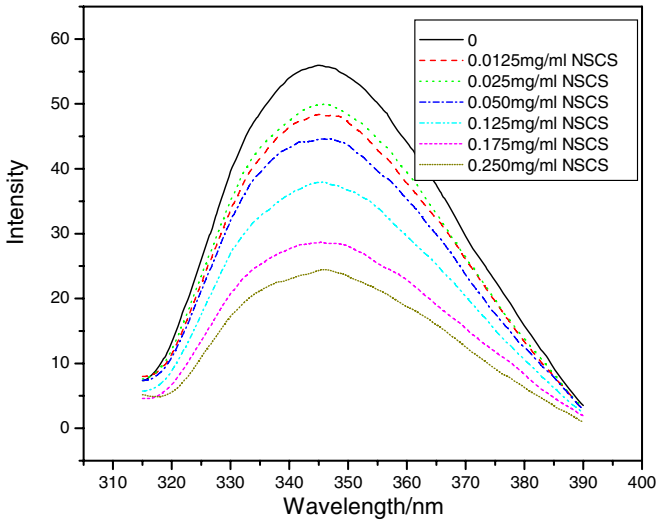

Fig. 2. Fluorescence spectrum of BSA in different concentrations of NSCS (BSA concentration was kept at 0.33 mg/ml).

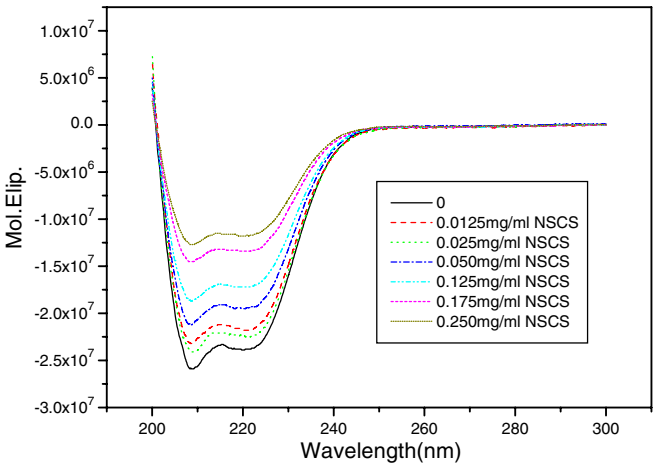

Fig. 3. Circular dichroism (CD) spectrum of BSA in different concentrations of NSCS (BSA concentration was kept at 0.33 mg/ml).

number and sequence of amino acid residues linked together by peptide bonds. The secondary structure is any such folding which is brought about by linking the carbonyl and amide groups of the backbone together by means of hydrogen bonds. There are three common secondary structures in proteins, namely α-helices, β-sheets, and turns. Those that cannot be classified as one of the standard three classes is usually grouped into a category called "random coil". Bovine serum albumin (BSA) is an ellipsoidal protein with the dimensions of $14 \times 4 \times 4$ nm. It consists of 582 amino acid residues and has a molecular weight of 66700 Da (Peters, 1985). The estimated percentages of α-helix and β-sheet contents from circular dichroism spectrum are listed in Table 1.

As shown in Table 1, the pure BSA has 30.6% α-helix and 14.9% β-sheet. The helix components become 34.6% and 34.3% in 0.0125 and 0.025 mg/ml of NSCS solution, respectively, and are higher than that of pure BSA. This result may be caused by the dissolution of BSA into the hydrophobic domain of NSCS. By further increasing the NSCS concentration, α-helix content decreases and becomes comparable with that of pure BSA. At the same time, the β-sheet component of BSA in the higher concentration of NSCS is similar to that of pure BSA, indicating the amide regions, normally assigned to protein secondary structure, were not significantly changed. As analyzed above, in the case of high concentration of NSCS, the complex formed between NSCS and BSA due to the chain entanglement. The present result suggests that the polypeptide backbone is not cleaved during the chain entanglement process and the side chain functional groups remain intact. BSA can retain its folded conformation in a NSCS matrix.

The magnitude of the interactions between protein molecules and polymeric systems in aqueous solutions determines the biocompatibility of the synthetic macromolecules. Thus, the blood and tissue compatibility of the synthetic macromolecules strongly depends on the conformational changes of the adsorbed and entrapped protein as well as on the stability of the polyelectrolyte complexes. Our present results demonstrate that a NSCS matrix can maintain the conformation of the encapsulated BSA, which is an excellent property to retain the activity of a bioactive drug or protein.

3.4. Isothermal titration calorimetric (ITC)

The interaction of BSA (1 mg/ml) with 0.025 mg/ml NSCS was studied. The calorimetry data for the experiment and the control titration of BSA into distilled water are plotted as observed molar enthalpy change (ΔH_{obs}) against BSA concentration in Fig. 4. The titration plot shows that each injection of BSA is accompanied by an exothermic enthalpy change (i.e., heat is released).

Calorimetric isotherms for NSCS–BSA interactions must be interpreted carefully, because ΔH_{obs} will represent the total enthalpy change for the process occurring in the sample cell. In the case of the NSCS–BSA systems, changes in enthalpy are likely to arise from a combination of binding and chain entanglements.

Usually, the control experiment for injection of a ligand into buffer will consist of a series of equal heats of dilution

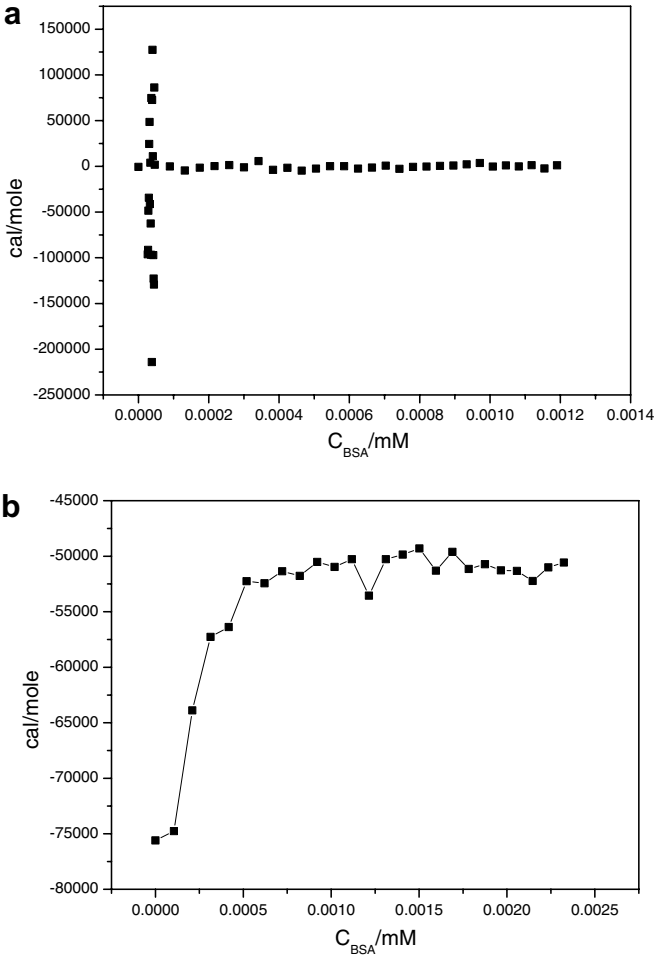

Fig. 4. Typical plot after integration of peak areas and normalization with respect to injectant concentration to yield a plot of molar enthalpy change (ΔH_{obs}) against BSA concentration (a) for the titration of 0.5 mg/ml of BSA into distilled water; (b) for the titration of 1 mg/ml of BSA into 0.025 mg/ml NSCS.

Table 1
α-Helix and β-sheet content dependence on the NSCS concentrations

NSCS concentration (mg/ml)	0 (%)	0.0125 (%)	0.025 (%)	0.05 (%)	0.125 (%)	0.175 (%)	0.25 (%)
α-Helix	30.60	34.60	34.30	31.80	31.90	31.70	31.60
β-Sheet	14.90	12.70	14.30	15.50	15.40	15.40	14.60

BSA concentration is kept at 0.33 mg/ml.

(O'Brien, Ladbury, & Chowdry, 2001). In this case, the BSA is injected from a concentrated solution in which the BSA molecules will tend to self-associate into aggregates due to their hydrophobicity. Therefore, when injected into distilled water, the BSA will undergo an endothermic (i.e., heat absorption) process of deaggregation, analogous to data for surfactant demicellization (Engberts & Blandamer, 2001). The extent of deaggregation will depend inversely on the concentration of BSA already present in the sample cell, because the BSA concentration in the cell will eventually exceed the critical aggregation concentration and subsequent enthalpy changes will correspond to dilution of BSA aggregates. Therefore, further injections will lead to the observation of progressively lower endothermic ΔH_{obs}. Fig. 4(a) shows typical plot after integration of peak areas and normalization with respect to injectant concentration to yield a plot of molar enthalpy change (ΔH_{obs}) against BSA concentration for the titration of 0.5 mg/ml of BSA into distilled water. It indicates that enthalpy change corresponding to dilution of BSA aggregates is as low as zero. As a result, it is not possible to determine a critical aggregation concentration from the calorimetry data.

Fig. 4(b) shows typical plot after integration of peak areas and normalization with respect to injectant concentration to yield a plot of molar enthalpy change (ΔH_{obs}) against BSA concentration for the titration of 1 mg/ml of BSA into 0.025 mg/ml NSCS. It demonstrates that the binding isotherms for the interactions between NSCS and BSA show obvious exothermic and then indicate a gradual decrease in exothermicity as BSA is titrated into the polymer solution until the saturation point is reached at 0.0005 mM of BSA, which converts to an approximate BSA/NSCS molar ratio of 30:1, assuming average molecular weights of 220,000 g/mol for NSCS and 66,000 g/mol for BSA. Injected BSA may cooperatively associate with NSCS-bound BSA or different sites on the NSCS.

Generally, charge binding, H-bonding, hydrophobic interactions and ion-exchange give rise to the exothermic contribution. As shown in Scheme 1, these are not groups that can be protonated or disassociated in NSCS macromolecule, and the titration is conducted in the distilled water, therefore the contributions of charge binding and ion-exchange can be excluded. Then H-bond and hydrophobic interactions should be the main driving force to form the chain entanglements between NSCS and BSA and give rise the exothermic contribution.

3.5. Morphology of NSCS encapsulated BSA

In our recent report (Zhu et al., 2006), NSCS is easy to aggregate into the regular sphere morphology with 50–100 nm in diameter. ITC studies imply that the existence stoichiometry binding between NSCS and BSA. We suppose that the precipitates will produce with increasing NSCS concentration due to the high entanglements of NSCS and BSA. Moreover, the saturation of binding sites is not necessary for precipitation to occur. BSA could cooperatively associate with NSCS chains by hydrophobic interactions and H-bonding. Fig. 5 shows the transmission electron microscopy (TEM) morphology (the molar ratio of BSA/NSCS was 30:1 and NSCS concentration was 0.5 mg/ml, respectively). Fig. 5(b) is the magnification of Fig. 5(a). From the Fig. 5, it can be shown clearly that complexes of NSCS and BSA also show regular sphere morphology with a diameter of 100–200 nm, which is bigger than that of NSCS aggregate in water. This is because of the chain entanglements of NSCS and BSA driven by the hydrophobic and H-bonding interactions.

3.6. The entrapment mechanism of BSA into NSCS

In the chitosan-based aqueous system, there are electrostatic interactions, hydrophobic interactions, and H-bonding, which will influence the solubility or assembly behaviors of chitosan and its derivatives (Zhu, Chan-Park, Dai, & Li, 2005). In the present system (Scheme 1), the amino groups of chitosan are transformed into –NH–CO–

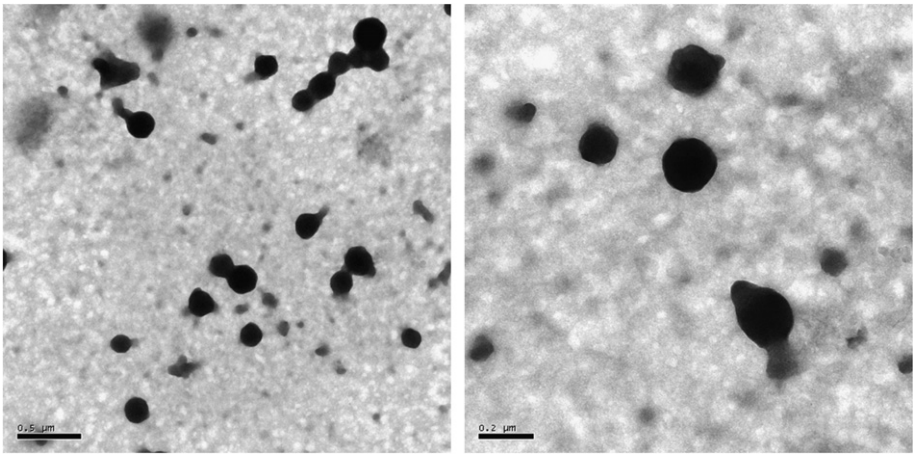

Fig. 5. TEM morphology of NSCS loaded BSA (molar ratio of BSA/NSCS was 30:1 and NSCS concentration was 0.5 mg/ml, respectively).

groups, and thus there are little groups that can protonated or dissociated in distilled water. Therefore, the electrostatic interactions are not the main factor for the formation of complexes of NSCS and BSA. NSCS has hydrophobic moieties such as $–CH_2CH_2–$, acetyl groups and glucosidic rings and BSA has hydrophobic residues of Trp, tyrosine and phenylalanine. Therefore, the hydrophobic associations should exist in NSCS/BSA systems as evidenced by fluorescence and ITC analysis. Moreover, there are also hydrophilic groups such as –NH–CO– and –OH groups in NSCS macromolecules and the polypeptide backbone of BSA, so the H-bond association is another important factor to drive the NSCS/BSA nanospheres to form. It is the hydrophobic and H-bond interactions that results in the chain entanglement between NSCS and BSA, which leads to the NSCS encapsulated BSA with larger diameters of nanospheres than that of self-aggregates of NSCS in distilled water. The conformation of BSA within a NSCS matrix does not change significantly, suggesting that NSCS is a kind of ideal matrix to load the hydrophilic and bioactive biomacromolecules.

4. Conclusions

In this study, the interactions between NSCS and BSA were studied in detail. ITC demonstrates that BSA binds to NSCS with a molar ratio of 30:1. The binding isotherms show exothermic, which is ascribed to the contributions of H-bond and hydrophobic interactions between BSA and NSCS. CD and Fluorescence spectrum indicates that the conformation of BSA can be maintained by the large within NSCS matrix. The NSCS can load BSA effectively due to the chain entanglement mechanism. The NSCS entrapped BSA shows nanosphere morphology with a 100–200 nm diameter at high concentration of NSCS revealed by TEM technique. This study demonstrates the potential of NSCS matrix for encapsulation of protein and other hydrophilic bioactive drugs.

Acknowledgments

This research was supported by a Natural and Scientific grant of Jiangsu Province, Project No. 05KJB430149 and Project BK2006072 (China).

References

Artursson, P., Lindmark, T., Davis, S. S., & Illum, L. (1994). Effect of Chitosanon on the permeability of monolayers of intestinal epithelial epithelial-cells (CACO-2). *Pharmaceutical Research, 11*, 1358–1361.

Borchard, G., Luessen, H. L., De Boer, A. G., Verhoef, J. C., Lehr, C. M., & Junginger, H. E. (1996). The potential of mucoadhesive polymers in enhancing intestinal peptide drug absorption. 3. Effects of chitosan-glutamate and carbomer on epithelial tight junctions in vitro. *Journal of Controlled Release, 39*, 131–138.

Calvo, P., Remunan-Lopez, C., Vila-Jato, J. L., & Alonso, M. J. (1997). Novel Hydrophilic chitosan-polyethylene oxide nanoparticles as protein carriers. *Journal of Applied Polymer Science, 63*, 125–132.

Chen, S. C., Wu, Y. C., Mi, F. L., Lin, Y. H., Yu, L. C., & Sung, H. W. (2004). A novel pH-sensitive hydrogel composed of *N*,*O*-carboxymethyl chitosan and alginate cross-linked by genipin for protein drug delivery. *Journal of Controlled Release, 96*, 285–300.

Dureja, H., Tiwary, A. K., & Gupta, S. (2001). Simulation of skin permeability in chitosan membranes. *International Journal of Pharmaceutics, 213*, 193–198.

Engberts, J. B. F. N., & Blandamer, M. J. (2001). Understanding organic reactions in water: from hydrophobic encounters to surfactant aggregates. *Chemical Communications, 18*, 1701–1708.

Gao, H., Wang, Y. N., Fan, Y. G., & Ma, J. B. (2006). Interactions of some modified mono-and bis-β-cyclodextrins with bovine serum albumin. *Bioorganic and Medicinal Chemistry, 14*, 131–137.

Greenfield, N., & Fasman, G. D. (1969). Computed circular dishroism spectra for evaluation of protein conformation. *Biochemistry, 8*, 4108–4116.

Guzman, M., Aberturas, M. R., Rodriguez-Puyol, M., & Molpeceres, J. (2000). Effect of nanoparticles on digitoxin uptake and pharmacologic activity in rat glomerular mesangial cell cultures. *Drug Delivery, 7*, 215–222.

Hu, Y., Jiang, X. Q., Ding, Y., Ge, H. X., Yuan, Y. Y., & Yang, C. Z. (2002). Synthesis and characterization of chitosan–poly(acrylic acid) nanoparticles. *Biomaterials, 23*, 3193–3201.

Iwasaki, N., Yamane, S. T., Majima, T., Kasahara, Y., Minami, A., Harada, K., et al. (2004). Feasibility of polysaccharide hybrid materials for scaffolds in cartilage tissue engineering: evaluation of chondrocyte adhesion to polyion complex fibers prepared from alginate and chitosan. *Biomacromolecules, 5*, 828–833.

Jelesarov, I., & Bosshard, H. R. (1999). Isothermal titration calorimetry and differential scanning calorimetry as complementary tools to investigate the energetics of biomolecular recognition. *Journal of Molecular Recognition, 12*, 3–18.

Jin, J., Song, M., & Hourston, D. J. (2004). Novel chitosan-based films cross-linked by genipin with improved physical properties. *Biomacromolecules, 5*, 162–168.

Kajihara, M., Sugie, T., Hojo, T., Maeda, H., Sano, A., Fujioka, K., et al. (2001). Development of a new drug delivery system for protein drugs using silicone (II). *Journal of Controlled Release, 73*, 279–291.

Kandori, K., Uoya, Y., & Ishikawa, T. (2002). Effects of acetonitrile on adsorption behavior of bovine serum albumin onto synthetic calcium hydroxyapatite particles. *Journal of Colloid and Interface Science, 252*, 269–275.

Kasai, S., Horie, T., Mizuma, T., & Awazu, S. (1987). Fluorescence energy transfer study of the relationship between the lone tryptophan residue and drug binding sites in human serum albumin. *Journal of Pharmaceutical Sciences, 76*(5), 387–392.

Kofuji, K., Ito, T., Murata, Y., & Kawashima, S. (2001). Biodegradation and drug release of chitosan gel beads in subcutaneous air pouches of mice. *Biological and Pharmaceutical Bulletin, 24*, 205–208.

Liang, H. F., Hong, M. H., Ho, R. M., Chung, C. K., Lin, Y. H., Chen, C. H., et al. (2004). Novel method using a temperature-sensitive polymer (methylcellulose) to thermally gel aqueous alginate as a pH-sensitive hydrogel. *Biomacromolecules, 5*, 1917–1925.

Liu, C. G., Desai, K. G. H., Chen, X. G., & Park, H. J. (2005). Preparation and characterization of nanoparticles containing trypsin based on hydrophobically modified chitosan. *Journal of Agricultural and Food Chemistry, 53*, 1728–1733.

Liu, W. G., Zhang, X., Sun, S. J., Sun, G. J., & Yao, K. D. (2003). *N*-alkylated chitosan as a potential nonviral vector for gene transfection. *Bioconjugate Chemistry, 14*, 782–789.

Magzoub, M., Kilk, K., Eriksson, L. E. G., Langel, U., & Graslund, A. (2001). Interaction and structure induction of cell-penetrating peptides in the presence of phospholipid vesicles. *Biochimica et Biophysica Acta, 1512*, 77–89.

Mao, H. Q., Roy, K., Troung-Le, V. L., Janes, K. A., Lin, K. Y., Wang, Y., et al. (2001). Chitosan-DNA nanoparticles as gene carriers: synthesis, characterization and transfection efficiency. *Journal of Controlled Release, 70*, 399–421.

Militello, V., Vetri, V., & Leone, M. (2003). Conformational changes involved in thermal aggregation processes of bovine serum albumin. *Biophysical Chemistry, 105*, 133–141.

O'Brien, R., Ladbury, J. E., & Chowdry, B. Z. (2001). Isothermal titration calorimetry of biomolecules. In S. E. Harding & B. Z. Chowdry (Eds.), *Protein-Ligand Interactions: Hydrodynamics and Calorimetry* (pp. 263–286). Oxford, U.K.: Oxford University Press.

Peng, Z. G., Hidajat, K., & Uddin, M. S. (2004). Conformational change of adsorbed and desorbed bovine serum albumin on nano-sized magnetic particles. *Colloids and Surfaces B: Biointerfaces, 33*, 15–21.

Peters, T. Jr., (1985). Serum-Albumin. *Advances in Protein Chemistry, 37*, 161–247.

Roy, K., Mao, H. Q., Huang, S. K., & Leong, K. W. (1999). Oral gene delivery with chitosan-DNA nanoparticles generates immunologic protection in a murine model of peanut allergy. *Nature Medicine, 5*, 387–391.

Soma, C. E., Dubernet, C., Bentolila, D., & Benita, S. (2000). Couvreur, P. Reversion of multidrug resistance by co-encapsulation of doxorubicin and cyclosporine A in polyalkylcynoacrylate nanoparticles. *Biomaterials, 21*, 1–7.

Walton, A. G., & Maenpa, F. C. (1979). Application of fluorescence spectroscopy to the study of proteins at interfaces. *Journal of Colloid and Interface Science, 72*(2), 265–278.

Wehrle, P., Magenheim, B., & Benita, S. (1995). The influence of process parameters on the PLA nanoparticle size distribution, evaluated by means of factorial design. *European Journal of Pharmaceutics and Biopharmaceutics, 41*, 19–26.

Wiseman, T., Williston, S., Brandts, J. F., & Lin, L. (1989). Rapid measurement of binding constants and heats of binding using a new titration calorimeter. *Analytical Biochemistry, 179*, 131–137.

Xu, Y. M., & Du, Y. M. (2003). Effect of molecular structure of chitosan on protein delivery properties of chitosan nanoparticles. *International Journal of Pharmaceutics, 250*, 215–226.

Zhu, A. P., Chan-Park, M. B., Dai, S., & Li, L. (2005). The aggregation behavior of *O*-carboxymethylchitosan in dilute solution Colloid and surface B. *Biointerfaces, 43*, 143–149.

Zhu, A. P., Chen, T., Yuan, L. H., Wu, H., & Lu, P. (2006). Synthesis and Characterization of *N*-succinyl-chitosan and its Self-assembly of Nanospheres. Carbohydrate Polymers, in press.